THREE-DIMENSIONAL FINITE ELEMENT ANALYSIS OF COMPOSITE LAMINATES SUBJECTED TO TRANSVERSE IMPACT

SURENDRA KUMAR AND B. PRADHAN*

*National Metallurgical Laboratory, Jamshedpur - 831 007. *Department of Mechanical Engineering, Indian Institute of Technology, Kharagpur - 721 302.*

Abstract

An interest in the low velocity impact problems has been revived with the advent of laminated composite materials and their increasing use in aerospace and other applications. The reason for this new activity is that despite certain advantages of these materials over more traditional materials, composites are known to be vulnerable to impact. Impacts may occur anywhere during manufacture, normal operations, or maintenance and may induce significant internal damage in the form of matrix cracking, delamination or fibre breakage, that are undetectable by visual inspection and cause significant reductions in the strength and stability of the structure.

In the present paper, a three-dimensional finite element and transient dynamic analysis of fibre-reinforced polymer matrix composite laminates (e.g. graphite/epoxy, glass/epoxy, etc.) subjected to transverse foreign object impact is performed. Layered version of eight-noded isoparametric brick element with incompatible modes is used to model the laminate. Transient dynamic equilibrium equation is integrated step-by-step with respect to time using Newmark direct time integration method. Non-linear contact law reported in literature is used to model the local contact behavior and the time-varying contact force is calculated based on the relative displacement between impactor and laminate using Newton-Raphson method. Based on the finite element model, a versatile computer software was developed in C++ programming language using object-oriented approach. The software can be used to determine several results such as contact force history, displacement and velocity histories of impactor and the time-varying displacements, forces, strains and stresses throughout the laminate. Some example problems are considered to study the effects of impactor velocity and laminate boundary conditions on impact behavior of graphite/epoxy composite laminates, and results are presented for time-history of contact force and laminate central deflection. The transient dynamic strains and stresses inside the laminate were also calculated for few cases

Introduction

An interest in the low velocity impact problems has been revived with the advent of laminated composite materials and their increasing use in aerospace and other applications. The reason for this new activity is that despite certain advantages of these materials over more traditional materials, composites are known to be vulnerable to impact. Impacts may occur anywhere during manufacture, normal operations, or maintenance and may induce significant internal damage in the form of matrix cracking, delamination or fibre breakage, that are undetectable by visual inspection and cause significant reductions in the strength and stability of the structure. In addition, the impact response and failure modes of composite laminates are greatly influenced by varying fundamental parameters such as fibre and matrix properties, fibre orientation, stacking sequence and laminate geometry.

It is, therefore essential to understand the impact response and damage mechanisms of composites and develop appropriate models for developing improved materials and design methods accounting for impact. Accordingly, numerous experimental and analytical investigations have been performed for this purpose and the summary of the work is reported in References [1,2].

It has generally been recognized since earlier work on impact of isotropic beams that an accurate account of contact behavior is one of most important steps in analyzing impact response problems. Sun and Chattopadhyay [3] used Hertzian contact law to analyze simply-supported laminated composite plate subjected to central impact of a mass. Yang and Sun [4] proposed a power law for graphite/epoxy composite laminate based on static indentation tests using steel balls as indentors. This contact law accounts for permanent indentation after unloading cycles. The modified version obtained by Tan and Sun [5] was used by several authors in their finite element approaches.

Several of these analyses were based on plate theories and couldn't provide information about stress and strain distributions, especially out-of-plane stresses, through the laminate thickness. This information is one of the initial steps to predict the impact damage in laminated composites [6,7].

In the present study, a three-dimensional finite element and transient dynamic analysis of graphite/epoxy composite laminates subjected to transverse impact is performed and implemented by a specially developed computer code. The objective of the analysis is to evaluate all the time-varying deformations, strains and stresses throughout the laminate. Effects of different parameters such as impactor velocity and laminate boundary conditions are investigated.

Contact Analysis

When a composite laminate is impacted by a mass, contact force results. The evaluation of the contact force depends on a contact law which relates the contact force F with the indentation depth α (the change in the distance between the center of the impactor's nose and the mid-surface of the laminate). In the present study, the modified version of Hertzian contact law proposed by Yang and Sun [4] based on static indentation tests is used as described below.

Loading :

$$F = k\alpha^{1.5} \tag{1}$$

Unloading :

$$F = F_m \left[\frac{\alpha - \alpha_o}{\alpha_m - \alpha_o} \right]^{2.5} \tag{2}$$

Reloading :

$$F = F_m \left[\frac{\alpha - \alpha_o}{\alpha_m - \alpha_o} \right]^{1.5} \tag{3}$$

where k is the modified constant of the Hertz contact theory defined by Yang and Sun [4] for a flat laminate as

$$k = \frac{4}{3} \sqrt{r_I} \frac{1}{\left[(1 - v_I^2)/E_I + 1/E_{yy} \right]} \tag{4}$$

where r_I, v_I, and E_I are the local radius, the Poisson's ratio, and the Young's modulus of the impactor respectively. E_{yy} is the transverse modulus normal to the fibre direction in the uppermost composite layer. F_m is the maximum contact force just before unloading, α_m is the indentation corresponding to F_m, and α_o is the permanent indentation during this loading-unloading process and can be determined from the following expressions

$$\alpha_o = 0 \qquad \text{when} \quad \alpha_m < \alpha_{cr}$$

$$\alpha_o = \alpha_m \left[1 - \left(\frac{\alpha_{cr}}{\alpha_m} \right)^{2/5} \right] \qquad \text{when} \quad \alpha_m \geq \alpha_{cr}$$

where α_{cr} is the critical indentation.

Finite Element Model

Governing Equations

The transient dynamic equilibrium equation neglecting damping is

$$[M]\{\ddot{u}\} + [K]\{u\} = \{F\}$$

where [M] and [K] are structural mass and stiffness matrices, $\{u\}$ and $\{\ddot{u}\}$ are the nodal displacement and acceleration vectors, and $\{F\}$ is the applied load vector.

Element Characteristics

In the present analysis, three-dimensional eight-noded isoparametric brick element is used (Fig. 1).

The shape functions defining the geometry and variation of displacements for this element is given by

$$N_i = \frac{1}{8}\left(1 + \xi\xi_i\right)\left(1 + \eta\eta_i\right)\left[1 + \zeta\zeta_i\right] \qquad (7)$$

where ξ, η and ζ are natural coordinates, and ξ_i, η_i and ζ_i are the values of natural coordinates for a node i.

To improve the accuracy in simulating flexural response, incompatible modes proposed by Wilson et al. [8,9] are added to the brick element shape functions. These modes are represented by the functions of the type

$$P_1 = \left(1 - \xi^2\right), \quad P_2 = \left(1 - \eta^2\right), \quad P_3 = \left(1 - \zeta^2\right) \quad (8)$$

The element mass and stiffness matrices are evaluated for this element as

$$\left[m^e\right] = \int_{-1}^{+1}\int_{-1}^{+1}\int_{-1}^{+1}[N]^T \rho[N]\det[J]d\xi d\eta d\zeta \qquad (9)$$

$$\left[k^e\right] = \int_{-1}^{+1}\int_{-1}^{+1}\int_{-1}^{+1}[B]^T[D][B]\det[J]d\xi d\eta d\zeta \qquad (10)$$

where [B] is the strain-displacement matrix and [J] is the jacobian matrix. The material density ρ and elasticity matrix [D] depend on the material properties and the orientations of the plies through the thickness of the element. Therefore, numerical integration in these equations must be carried out from ply to ply through the element thickness. By this way, several plies can be grouped into an element, resulting in a significant reduction in computational time and memory space.

Newmark Direct Integration Method

In order to integrate finite element equation of motion (eqn (6)) step-by-step with respect to time, Newmark Direct Integration Method is used. The method may be briefly introduced as follows

It is assumed that [10]

$$\{\dot{u}_{n+1}\} = \{\dot{u}_n\} + \left[(1-\alpha)\{\ddot{u}_n\} + \alpha\{\ddot{u}_{n+1}\}\right]\Delta t \tag{11}$$

$$\{u_{n+1}\} = \{u_n\} + \{\dot{u}_n\}\Delta t + \left[\left[\frac{1}{2} - \beta\right]\{\ddot{u}_n\} + \beta\{\ddot{u}_{n+1}\}\right](\Delta t)^2 \tag{12}$$

where Δt is the time step, n is the step number, and the parameters α and β can be determined to obtain integration accuracy and stability.

Eqn (12) is now rearranged and substituted into eqn (6) evaluated at time t_{n+1} to form:

$$[\hat{K}]\{u_{n+1}\} = \{\hat{F}_{n+1}\} \tag{13}$$

where,

$$[\hat{K}] = [K] + a_o[M] \tag{14}$$

$$\{\hat{F}_{n+1}\} = \{F_{n+1}\} + [M](a_o\{u_n\} + a_1\{\dot{u}_n\} + a_2\{\ddot{u}_{n+1}\}) \tag{15}$$

In eqns (14) and (15),

$$a_o = \frac{1}{\beta(\Delta t)^2}, \quad a_1 = \frac{1}{\beta(\Delta t)}, \quad a_2 = \frac{1}{2\beta} - 1$$

Once the displacements $\{u_{n+1}\}$ at time $\{t_{n+1}\}$ are obtained by solving eqn (13), the velocities $\{\dot{u}_{n+1}\}$ and accelerations $\{\ddot{u}_{n+1}\}$ are computed using eqns (11) and (12) respectively.

Results and Discussion

Based on the finite element model described above, a versatile computer program is developed in C++ object-oriented programming language under UNIX environment. The software can be used to provide solutions for a wide range of problems of composite laminates of different geometry and ply orientations subjected to transverse impact with or without any preload. Several results, such as contact force history, displacement and velocity histories of the center-point of impactor, and the time-varying displacements, forces, strains and stresses throughout the laminate can be generated.

The problem description for a rectangular laminated plate is shown in Fig.2. Impactor is assumed to move in the + ve z-direction and the impacted side is the first layer in the stacking sequence. Depending upon the geometry, loading, material properties and orientations of the plies, a full model or a quarter model of the laminate is analyzed. However, the finite element model is always kept in the first quadrant of the coordinate system. A typical finite element mesh for one quarter of the plate is shown in Fig.3.

In order to validate the model and the computer code, results from the present analysis are compared with analytical solutions. An isotropic rectangular steel plate of length 200 mm, width 200 mm and thickness 8 mm simply supported on its edges is considered. The plate is subjected to an impact induced by a 20 mm diameter steel ball with initial velocity 1 m/s. The present FEM solutions for the contact force and displacements of the impactor and centre of the plate are compared with the analytical solutions [11]. As shown from Figs 4(a) and 4(b), an excellent agreement exists between the two solutions.

Next, the impact response of the rectangular graphite/epoxy plate with a ply

orientation of $[0/-45/45/90]_{2s}$ is investigated. The plate of length 76.2 mm and width 76.2 mm clamped on its edges is impacted by an aluminium sphere of 12.7 mm diameter travelling at three different velocities of 12.7 m/s, 25.4 m/s and 38.1 m/s. The material properties of fiberite T300/934 graphite/epoxy composite are listed in Table 1. The results of contact force and displacements of the centre of the plate are presented in Fig. 5. It is worth noting that during impact, the contact force is reduced to zero for a certain period of time, indicating that the impactor is not in continuous contact with the plate. At some time after the first contact the plate centre moves away from the impactor, and the plate and the impactor separate. The plate and the impactor come in contact again after the plate reverses its direction of motion and snaps back. It can also be observed that as the velocity increases, contact force increases for both contacts while the contact duration remains approximately the same.

The above results for simply-supported boundary conditions are presented in Fig.6. A comparison of Fig.6 with Fig.5 reveals that the maximum contact force for both the clamped and simply-supported plate problems is very similar, but the contact duration is longer for the simply-supported condition than the clamped condition. Also the second contact occurs much later for the simply-supported condition. The increase in flexibility due to the simply-supported edges is responsible for these phenomena.

The present computer code is also capable of determining time-varying strains and stresses throughout the composite laminate. Figs 7 and 8 show all the six components of the time-varying strains and stresses at certain locations of the laminate for clamped boundary condition and impactor velocity of 25.4 m/s. These locations are at a distance approximately 8 mm from the centre of the laminate along the diagonal line and at the top of 2nd, 6th, 10th and 14th plies of the laminate. As can be seen from these figures, the strains and stresses fluctuate about zero and are sometimes tensile and sometimes compressive.

Once the states of strain and stress inside the laminate are known at any time point, appropriate failure criteria may be applied to predict the initiation of impact damage in the form of matrix cracking and delamination.

Conclusion

Transient dynamic analysis of composite laminates subjected to transverse foreign object impact has been performed using three-dimensional finite element method and based on the model, a special computer code in C++ is developed and successfully validated. Some example problems have been considered to study the impact response of composite laminates. Effects of different impactor velocities and laminate boundary conditions are investigated. Results are presented for contact force and lami-

nate central displacement as functions of time. Time-varying strains and stresses inside the laminate have also been calculated for few problems. From the results, several important points are demonstrated.

Since the present model is capable of determining time-varying strains and stresses throughout the laminate, it can easily be extended to predict the initiation of impact damage in the form of matrix cracking and delamination using appropriate failure criteria.

References

1   Abrate, S., Impact on laminated composite materials, Applied Mechanics Review, **44** (1991) 155-190.

2   Cantwell, W.J. and Morton, J., The impact resistance of composite materials - a review. Composites, **22** (1991) 347-362.

3   Sun, C.T. and Chattopadhyay, S., Dynamic response of anisotropic laminated plates under initial stress to impact of a mass, Journal of Applied Mechanics, **42** (1975) 693-698.

4   Yang, S.H. and Sun, C.T., Indentation law for composite laminates, ASTM STP 787, 1982, 425-449.

5   Tan, T.M. and Sun, C.T., Use of statical indentation laws in the impact analysis of laminated composite plates, Journal of Applied Mechanics, **52** (1985) 6-12.

6   Wu, H.T. and Chang, F.K., Transient dynamic analysis of laminated composite plates subjected to   transverse impact, Computers and Structures, **31** (1989) 453-466.

7   Choi, H.Y. and Chang, F.K., A model for predicting damage in graphite/epoxy laminated composites from low-velocity point impact, Journal of Composite Materials, **26** (1992) 2134-2169.

8   Wilson, E.L., Taylor, R.L., Doherty, W.P., and Ghaboussi, J., Incompatible displacement models. In Fenves, S.J., Perrone, N., Robinson, A.R., and Schnobrich, W.C., eds., Numerical and Computer Methods in Structural Mechanics, Academic Press, New York, 1973, pp. 43-57.

9   Taylor, R.L., Beresford, P.J., and Wilson, E.L., A non-conforming element for stress analysis, International Journal for Numerical Methods in Engineering, **10** (1976) 1211-1219.

10 Bathe, K.J., Finite Element Procedures in Engineering Analysis, Prentice-Hall of India, New Delhi, 1990.

11 Goldsmith, W., Impact: The Theory and Physical Behavior of Colliding Solids, Edward Arnold Ltd., London, 1960.

Table 1
Material Properties of Fiberite T300/934 Graphite/Epoxy [6]

Ply thickness, t	6.250×10^{-3} in†
Density, ρ	5.548×10^{-2} lbm/in³ ✚
Critical indentation, α_{cr}	3.160×10^{-3} in
Longitudinal Young's modulus, E_{xx}	2.109×10^{7} psi ✳
Transverse Young's modulus, E_{yy}	1.450×10^{6} psi
Shear modulus in x-y direction, G_{xy}	8.251×10^{5} psi
Poisson's ratio in x-y direction, ν_{xy}	0.3
Poisson's ratio in y-z direction, ν_{yz}	0.3

† 1 in = 25.4mm
✚ 1lbm/in³ = 2.768 x 10⁴ kg/m³
✳ 1 psi = 6.895 x 10³ Pa
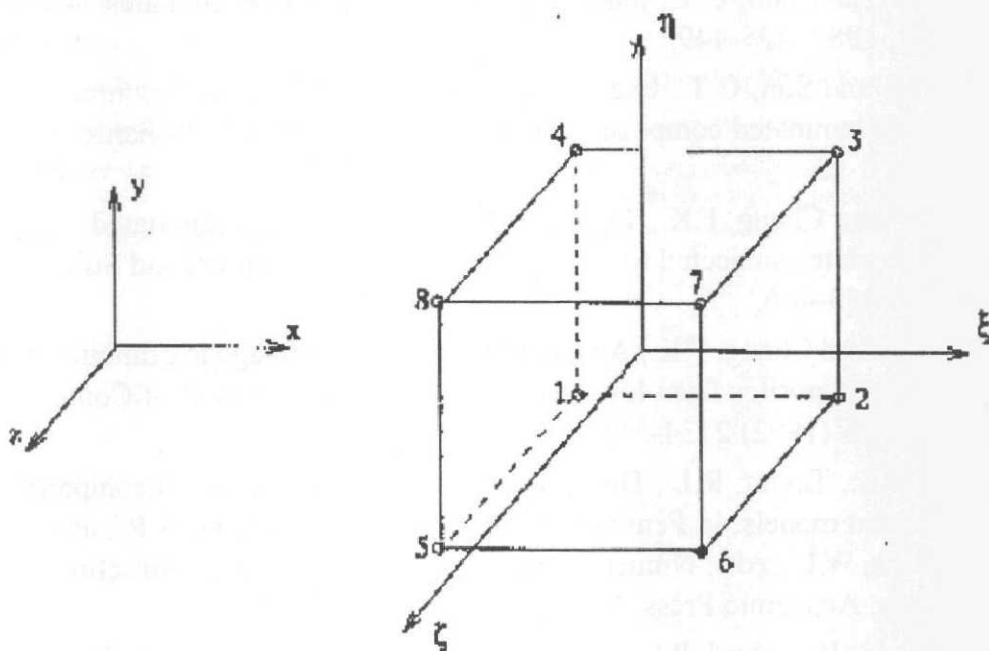
Fig. 1 - Eight-noded brick element.

MASS, m
NOSE RADIUS, R
INITIAL VELOCITY, V_0

BOUNDARIES:
SIMPLY-SUPPORTED
OR CLAMPED.
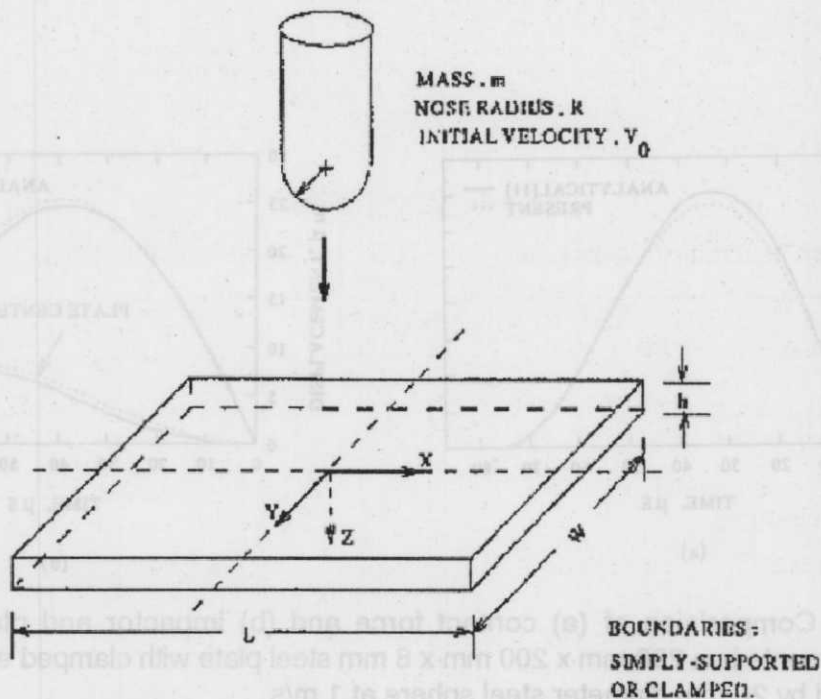
Fig. 2 - Configuration of rectangular laminated plate subjected to transverse
impact of a solid object.

TIME-VARYING
CONTACT FORCE

LAYERED ELEMENTS
THROUGH THE THICKNESS
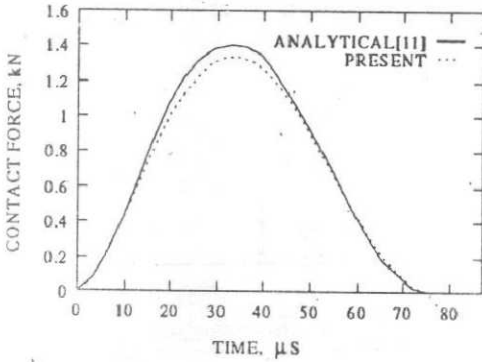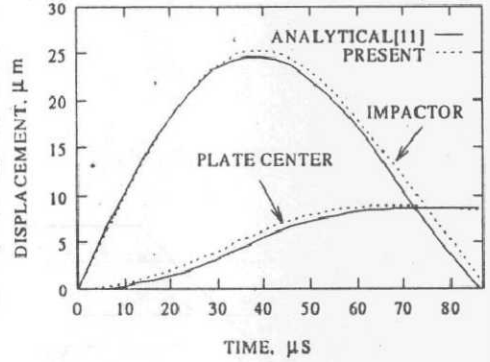
PLIES OF DIFFERENT THICKNESSES
AND FIBRE ORIENTATIONS
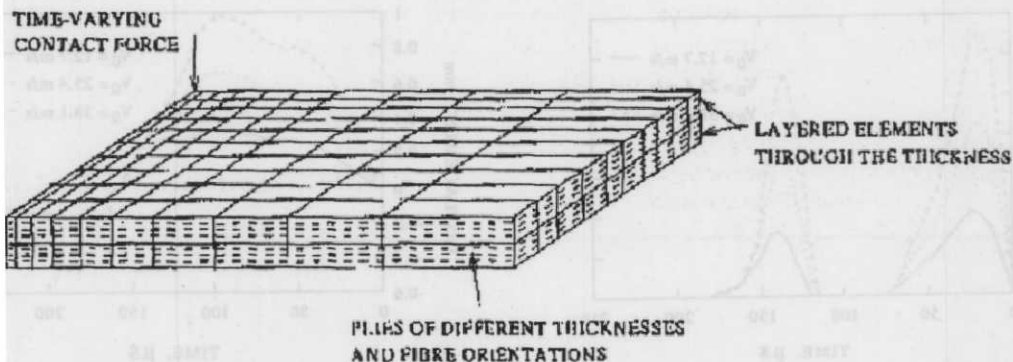
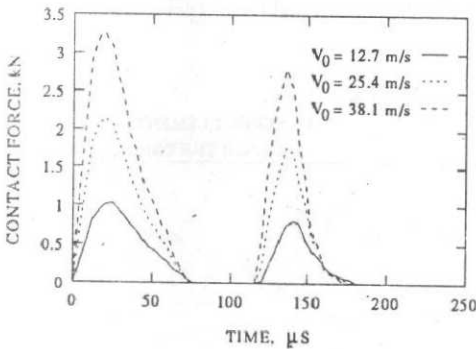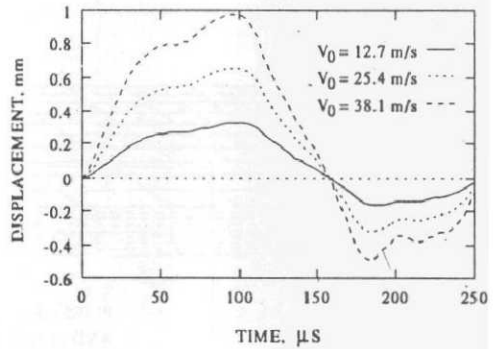Fig. 3 - A typical finite element mesh for one-quarter of the plate.

Fig. 4 - Comparision of (a) contact force and (b) impactor and plate center displacements in a 200 mm x 200 mm x 8 mm steel plate with clamped edges impacted by 20 mm diameter steel sphere at 1 m/s.

Fig. 5 - (a) contact force and (b) plate center displacement in a 76.2 by 76.2 mm T300/ 934 graphite/epoxy plate ($[0/-45/45/90]_{2s}$) with clamped edges impacted by 12.7 mm diameter aluminium sphere at 12.7, 25.4, and 38.1 m/s.
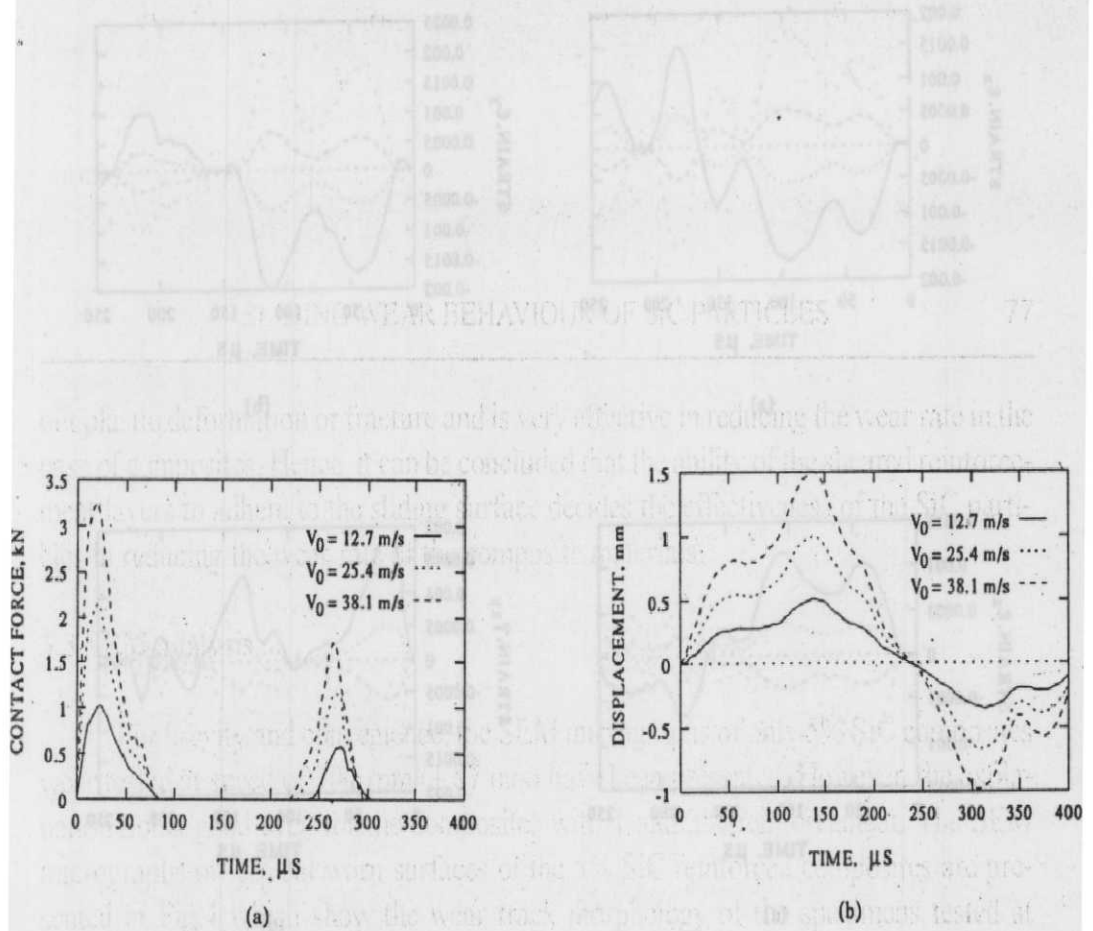
Fig. 6 - (a) contact force and (b) plate center displacement in a 76.2 by 76.2 mm T300/934 graphite/epoxy plate ([0/−45/45/90]$_{2s}$) with simply supported edges impacted by 12.7 mm diameter aluminium sphere at 12.7, 25.4, and 38.1 m/s.
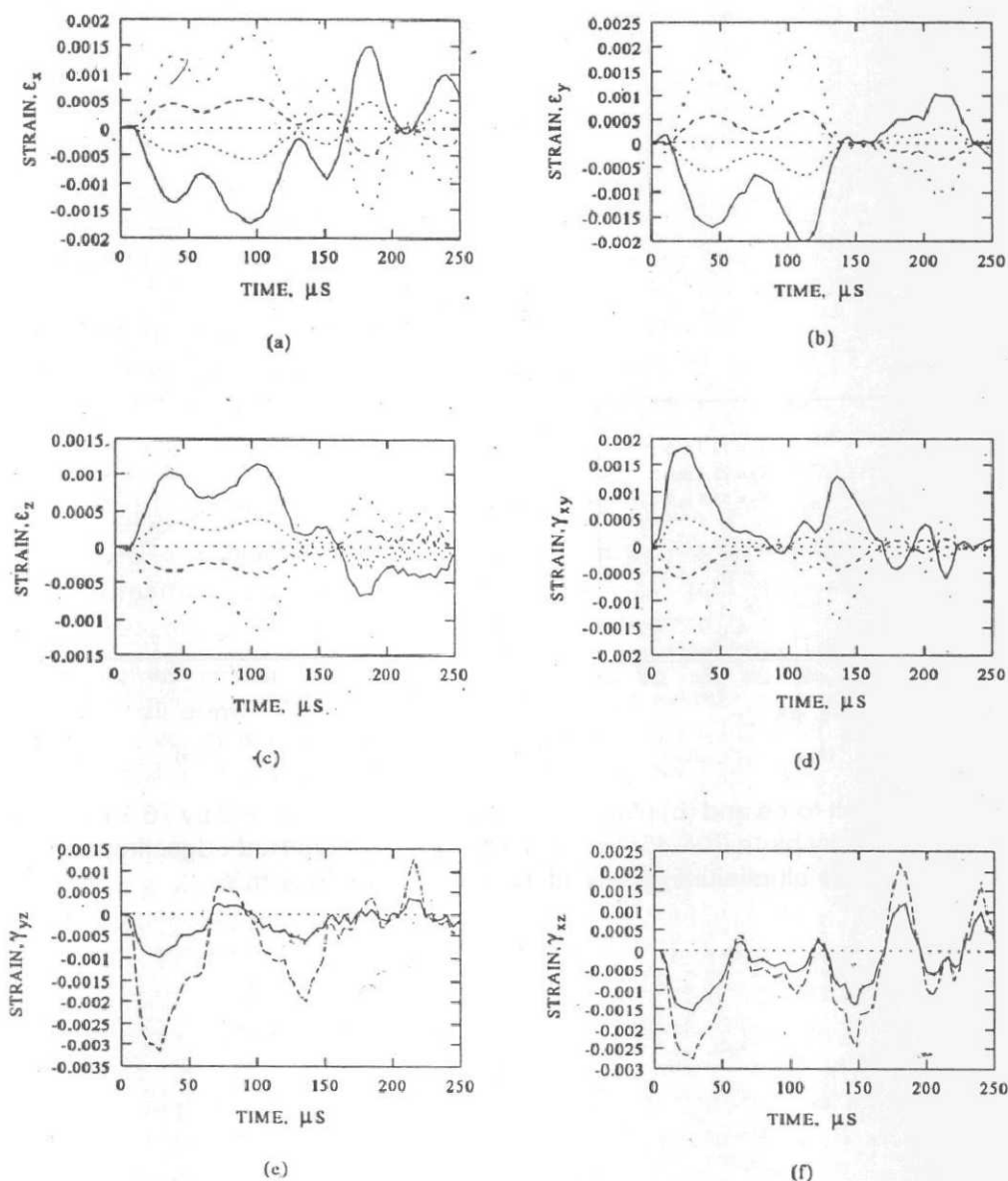
Fig. 7 - The six components of strains at a point 8 mm away from the centre of the plate along the diagonal line and at the top of 2nd (——), 6th (··········) , 10th (-------) and 14th (········) plies of a 76.2 by 76.2 mm T300/934 graphite/epoxy plate ([0/–45/45/90]$_{2s}$) with clamped edges impacted by 12.7 mm diameter aluminium sphere at 25.4 m/s. (In Figs (e) & (f), shear strains γ_{yz} and γ_{xz} are identical for 2nd & 14th plies and 6th & 10th plies.)
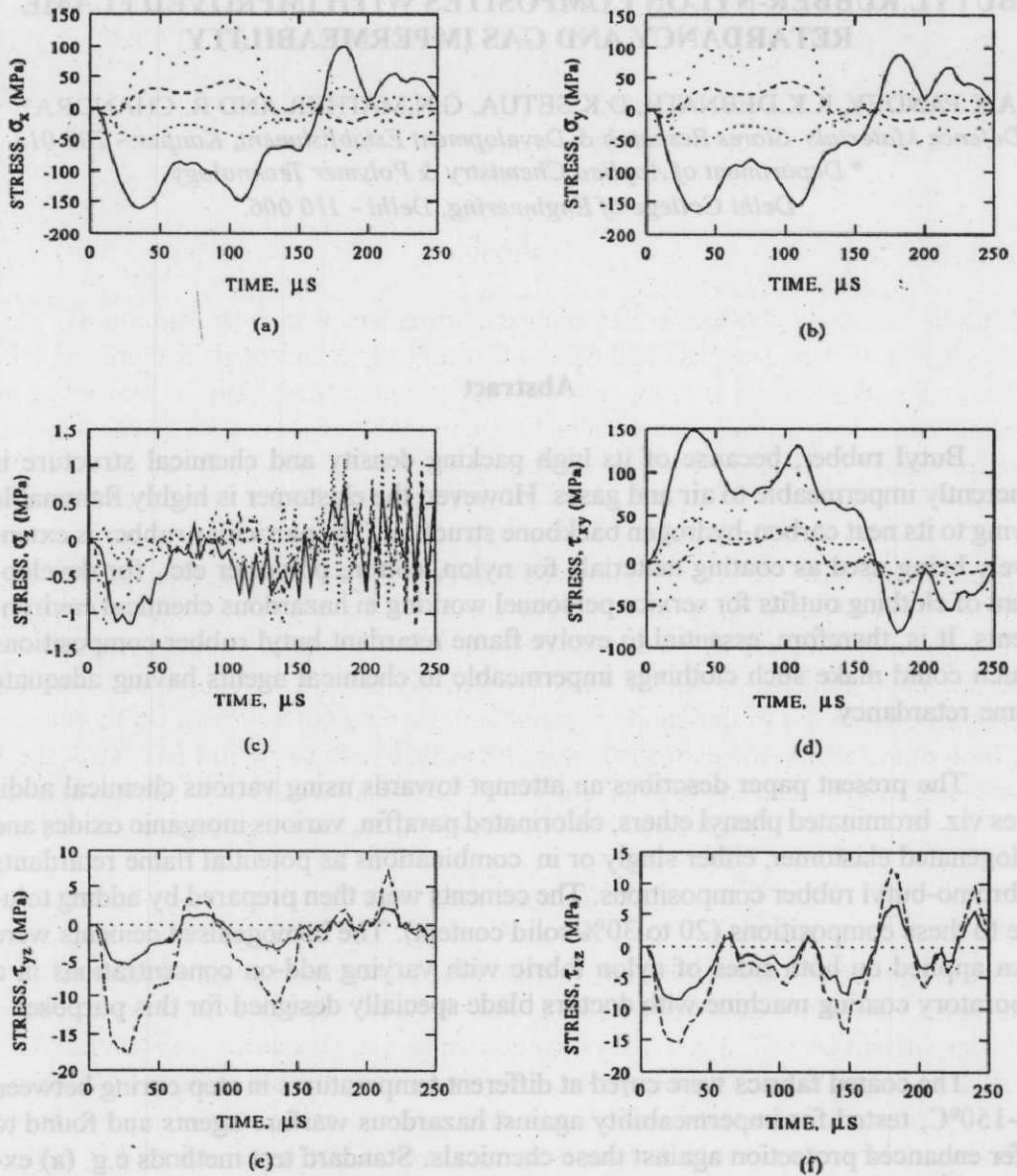
Fig. 8 - The six components of stresses at a point 8 mm away from the centre of the plate along the diagonal line and at the top of 2nd (———), 6th (············) , 10th (-------) and 14th (········) plies of a 76.2 by 76.2 mm T300/934 graphite/epoxy plate ([0/−45/45/90]$_{2s}$) with clamped edges impacted by 12.7 mm diameter aluminium sphere at 25.4 m/s. (In Figs (e) & (f), shear stresses τ_{yz} and τ_{xz} are identical for 2nd & 14th plies and 6th & 10th plies.)